Whole-Body Subcellular Multicolor Imaging of Tumor-Host Interaction and Drug Response in Real Time

Meng Yang,[1] Ping Jiang,[1] and Robert M. Hoffman[1,2]

[1]AntiCancer, Inc. and [2]Department of Surgery, University of California, San Diego, California

Abstract

To noninvasively image cancer cell/stromal cell interaction in the tumor microenvironment and drug response at the cellular level in live animals in real time, we developed a new imageable three-color animal model. The model consists of green fluorescent protein (GFP)–expressing mice transplanted with dual-color cancer cells labeled with GFP in the nucleus and red fluorescent protein in the cytoplasm. The Olympus IV100 Laser Scanning Microscope, with ultra-narrow microscope objectives ("stick objectives"), is used for three-color whole-body imaging of the two-color cancer cells interacting with the GFP-expressing stromal cells. In this model, drug response of both cancer and stromal cells in the intact live animal is also imaged in real time. Various *in vivo* phenomena of tumor-host interaction and cellular dynamics were imaged, including mitotic and apoptotic tumor cells, stromal cells interacting with the tumor cells, tumor vasculature, and tumor blood flow. This new model system enables the first cellular and subcellular images of unperturbed tumors in the live intact animal. New visible real-time targets for novel anticancer agents are provided in this model, including the color-coded interacting cancer and stromal cells, tumor vasculature, and blood flow. This imageable model should lead to many new insights of *in vivo* cancer cell biology and to novel drug discovery. [Cancer Res 2007; 67(11):5195–200]

Introduction

Fluorescent proteins can be used to visualize primary tumor growth, tumor cell motility and invasion, metastatic seeding and colonization, angiogenesis, and the interaction between the tumor and its microenvironment (tumor-host interaction; refs. 1–6). Fluorescent proteins of many different colors have now been characterized, and these can be used to color-code cancer cells of a specific genotype or phenotype. For example, the behavior of highly metastatic cancer cells labeled with green fluorescent protein (GFP) and low metastatic cancer cells labeled with red fluorescent protein (RFP) can be directly compared *in vivo* (7). Alternatively, the host and the tumor can be differentially labeled with fluorescent proteins. For example, a transgenic mouse expressing GFP in all of its cells, or in specific cells such as endothelial cells, transplanted with tumor cells expressing RFP enables the interaction between the tumor cells and the host cells to be visualized in real time (8, 9). Real-time tracking of tumor growth and metastasis can be carried out in the intact animal (1, 6). For single-cell resolution, reversible acute skin flaps have been used over many parts of the body (skin, brain, lung, liver, etc.; ref. 10). Real-time imaging with fluorescent proteins is especially important when evaluating the efficacy of therapeutics on metastasis and tumor recurrence (11, 12).

Fluorescent proteins have very high extinction coefficients ranging from 6,500 up to ~95,000 (13). In addition, they have very high quantum yields ranging from 0.24 up to 0.8 (14). These properties make fluorescent proteins very bright. The large two-photon absorption of GFP is important for *in vivo* applications (14). Another important feature is the spectral distinction between many members of the family of fluorescent proteins; thus, a set of multicolor fluorescent proteins can be used simultaneously for multifunctional *in vivo* imaging. These properties make fluorescent proteins optimal for cellular imaging *in vivo*.

Our laboratory pioneered the use of GFP for *in vivo* imaging in 1997 (5). With the use of GFP, individual cancer cells could be observed in fresh unstained tissue or even the live animal for the first time. In 2000, we showed that GFP could be used for whole-body imaging (6). The present report shows the use of GFP as well as RFP to whole-body image color-coded interacting cancer and stromal cells.

Cancer cells coexist in a complex association with host-stromal tissue cells. The stroma provides the vascular supply to the tumor in the angiogenesis process as well as many other cell types and functions. The factors that regulate the development of the stromal elements, as well as the influences these constituents have on the tumor, are poorly understood. The lack of information about the interaction between tumor and stroma can be attributed in part to lack of suitable models (15). Tumor progression is a multistep process accompanied by the accumulation of mutations in cancer cells. However, it is now becoming clear that the tumor microenvironment is also critical for malignancy, which is in part the product of interaction between different cancer and host cell types (16).

The heterogeneous and structurally complex nature of the interactive tumor microenvironment is little understood. The relative amount of stroma and its composition vary considerably from tumor to tumor and vary within a tumor over the course of tumor progression. The interaction between cancer cells and stromal cells largely determines the phenotype of the tumor. For example, recent studies have shown that the growth, invasiveness, and angiogenesis of human breast tumor xenografts in mice depend on the presence of stromal fibroblasts (17).

The tumor microenvironment is a potential therapeutic target. Advantages to targeting the stroma cells are that the cells are genetically stable unlike cancer cells and are therefore less likely to develop drug resistance (18, 19). For example, anti–vascular endothelial growth factor antibodies, which inhibit formation of new blood vessels in the tumor, are used to treat colorectal cancer (20).

Note: Supplementary data for this article are available at Cancer Research Online (http://cancerres.aacrjournals.org/).

Requests for reprints: Robert M. Hoffman, AntiCancer, Inc., San Diego, CA 92111. Phone: 858-654-2555; Fax: 858-268-4175; E-mail: all@anticancer.com.

©2007 American Association for Cancer Research.

doi:10.1158/0008-5472.CAN-06-4590

We developed a simple yet powerful technique for delineating the morphologic events of tumor-induced angiogenesis and other tumor-induced host processes with dual-color fluorescence. The method clearly imaged implanted tumors and adjacent stroma, distinguishing unambiguously the host and tumor-specific components of the malignancy in fresh tissue samples. The dual-color fluorescence imaging was effected by using RFP-expressing tumors growing in transgenic mice that express GFP in essentially all nucleated cells. This model showed with great clarity the details of the tumor-stroma interaction, especially tumor-induced angiogenesis and tumor-infiltrating lymphocytes (8).

To noninvasively visualize cellular and subcellular events in the tumor microenvironment in real time in the live mouse, we used a laser scanning microscope with a 0.3-mm-diameter stick objective that is up to 2 cm in length. The system allows an imaging depth that extends to at least 200 μm. This novel imaging system, coupled with the use of the dual-color cancer cells and transgenic GFP mouse, has enabled noninvasive *in vivo* imaging of the cancer and stromal cells in the tumor microenvironment at the subcellular level, the subject of the current report.

Materials and Methods

Production of RFP retroviral vector. For RFP retrovirus production, the *Hin*dIII/*Not*I fragment from pDsRed2 (Clontech Laboratories, Inc.), containing the full-length RFP cDNA, was inserted into the *Hin*dIII/*Not*I site of pLNCX2 (Clontech Laboratories) that has the neomycin resistance gene to establish the pLNCX2-DsRed2 plasmid. PT67, an NIH3T3-derived packaging cell line (Clontech Laboratories) expressing the 10 Al viral envelope, was cultured in DMEM (Irvine Scientific) supplemented with 10% heat-inactivated fetal bovine serum (FBS; Gemini Bio-products). For vector production, PT67 cells, at 70% confluence, were incubated with a precipitated mixture of LipofectAMINE reagent (Life Technologies, Inc., Grand Island, NY) and saturating amounts of pLNCX2-DsRed2 plasmid for 18 h. Fresh medium was replenished at this time. The cells were examined by fluorescence microscopy 48 h after transduction. For selection of a clone producing high amounts of a RFP retroviral vector (PT67-DsRed2), the cells were cultured in the presence of 200 to 1,000 μg/mL G418 (Life Technologies) for 7 days (7).

Production of histone H2B-GFP vector. The histone *H2B* gene has no stop codon, thereby enabling the ligation of the *H2B* gene to the 5′-coding region of the *Aequoria victoria EGFP* gene (Clontech Laboratories). The histone *H2B-GFP* fusion gene was then inserted at the *Hin*dIII/*Cla*I site of the pLHCX (Clontech Laboratories) that contains the hygromycin resistance gene. To establish a packaging cell clone producing high amounts of a histone H2BGFP retroviral vector, the pLHCX histone H2B-GFP plasmid was transfected in PT67 cells using the same methods described above for PT67-DsRed2. The transfected cells were cultured in the presence of 200 to 400 μg/mL hygromycin (Life Technologies) for 15 days to establish stable PT67 H2B-GFP packaging cells (7).

RFP gene transduction of cancer cells. For RFP gene transduction, 70% confluent mouse mammary tumor (MMT) cells or Lewis lung carcinoma (LLC) cells were used. To establish dual-color cells, clones of cancer cells expressing RFP in the cytoplasm were initially established. In brief, cancer cells were incubated with a 1:1 precipitated mixture of retroviral supernatants of PT67-RFP cells and RPMI 1640 (Mediatech, Inc.) containing 10% FBS for 72 h. Fresh medium was replenished at this time. Cells were harvested with trypsin/EDTA 72 h after transduction and sub-

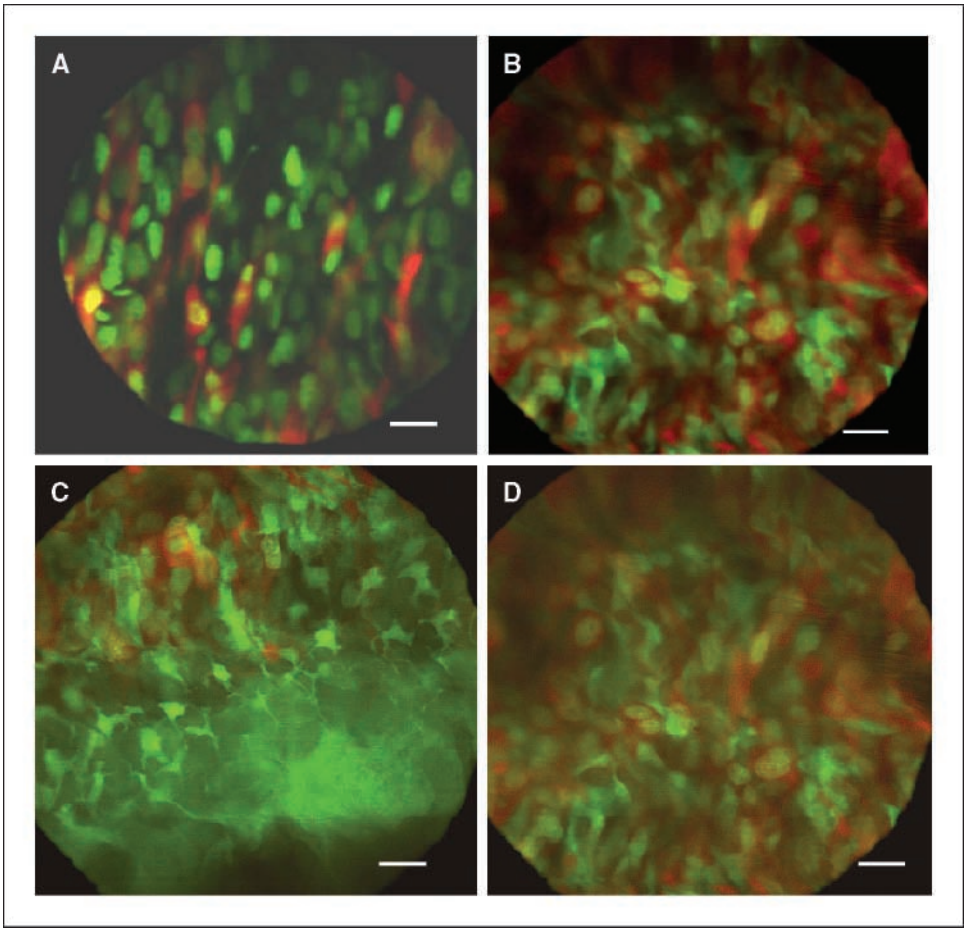

Figure 1. Whole-body, noninvasive, three-color subcellular imaging of cancer cell/stromal cell interaction in the live GFP mouse. *A,* whole-body image of cancer cell/stromal cell interaction of dual-color MMT mouse mammary cancer cells. *B,* whole-body image of cancer cell/stromal cells interaction of dual-color LLC cells. Dual-color cancer cells were injected in the footpad of the GFP transgenic nude mice. Whole-body images were acquired with the Olympus IV100 laser scanning microscope using the 3-mm stick objective 14 d after cell injection. The Olympus IV100 was also used for whole-body optical sectioning at 10 μm per section. *C*, a section 30 μm from the surface of the Lewis lung tumor. *D*, a section 80 μm from the surface. Note the interdispersal of the dual-color cancer cells among the GFP host stromal cells. *Bar,* 20 μm.

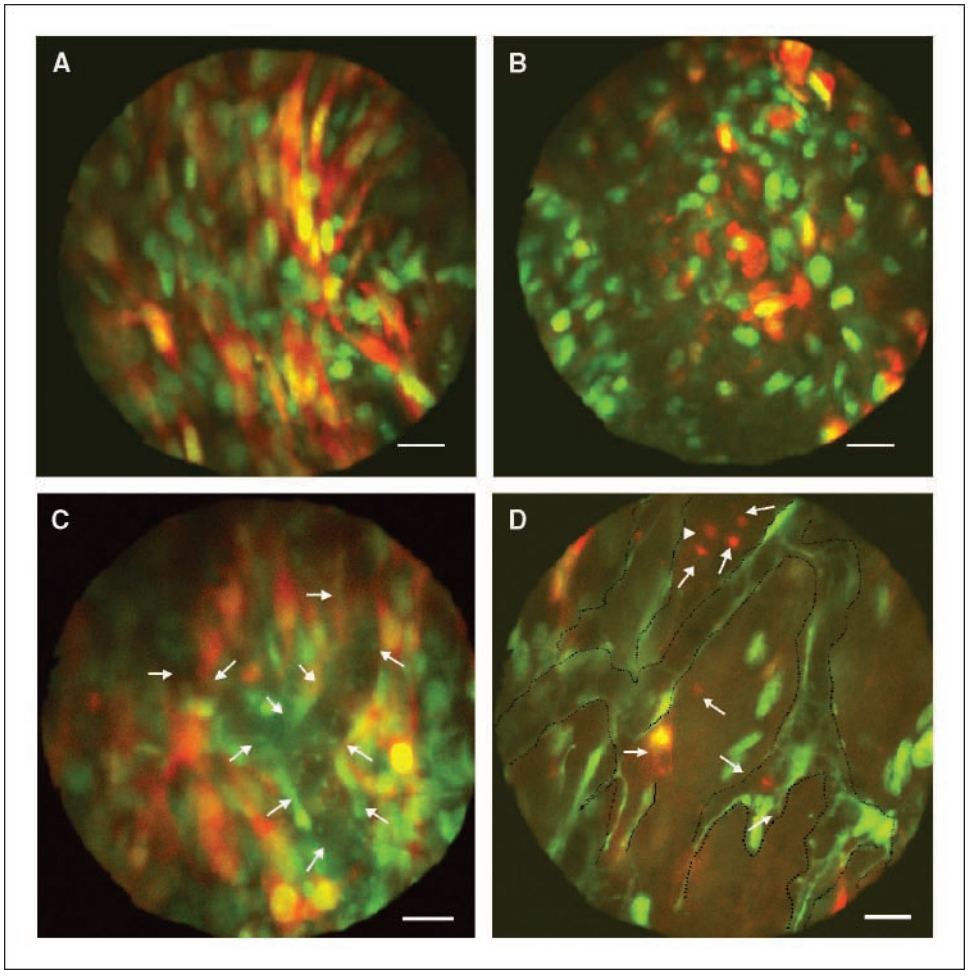

Figure 2. Whole-body, noninvasive, subcellular imaging of drug response of dual-color mouse mammary cancer cells and GFP stromal cells in the live GFP nude mouse with and without doxorubicin. Dual-color MMT cells were injected in the footpad of GFP transgenic nude mice as described in Fig. 1. *A,* whole-body image of untreated dual-color MMT cells in the footpad of a live GFP mouse. Note the numerous spindle-shaped dual-color MMT cells interdispersed among the GFP host cells. *B,* whole-body image of MMT dual-color cancer cells in a live GFP nude mouse 12 h after treatment with doxorubicin (10 mg/kg). The cancer cells lost their spindle shape, and the nuclei appear contracted. *C,* whole-body image of dual-color MMT tumor. Numerous dual-color spindle-shaped MMT cells interacted with GFP-expressing host cells. Well-developed tumor blood vessels and real-time blood flow were visualized by whole-body imaging (*arrows*). *D, in vivo* drug response of dual-color MMT tumor 12 h after i.v. injection of 10 mg/kg doxorubicin. All of the visible MMT cells lost their spindle shape. Many of the cancer cells fragmented (*arrows*). Tumor blood vessels were damaged (*dashed black lines*), and the number of cancer cells was dramatically reduced 12 h after chemotherapy. *Bar,* 20 μm.

cultured at a ratio of 1:15 in selective medium, which contained 200 μg/mL G418. The level of G418 was increased stepwise up to 800 μg/mL. RFP-expressing cancer cells were isolated with cloning cylinders (Bel-Art Products) using trypsin/EDTA and amplified by conventional culture methods (7).

Establishment of dual-color cancer cells. For establishing dual-color cells, RFP-expressing cancer cells were then incubated with a 1:1 precipitated mixture of retroviral supernatants of PT67 H2B-GFP cells and culture medium. To select the double transformants, cells were incubated with hygromycin 72 h after transfection. The level of hygromycin was increased stepwise up to 400 μg/mL. Clones of dual-color cancer cells were isolated with cloning cylinders under fluorescence microscopy. These clones were amplified by conventional culture methods. These sublines stably expressed GFP in the nucleus and RFP in cytoplasm (7).

Transgenic GFP nude mice. Transgenic C57/B6-GFP mice were originally obtained from Prof. Masaru Okabe (Research Institute for Microbial Diseases, Osaka University, Osaka, Japan). C57/B6-GFP mice express GFP under the control of the chicken β-actin promoter and cytomegalovirus enhancer. All of the tissues from this transgenic line, with the exception of erythrocytes and hair, express GFP. Ten-week-old transgenic GFP female C57/B6 mice were crossed with 6- to 8-week-old BALB/c *nu/nu* or NCR *nu/nu* male mice (Harlan). Male F_1 mice were crossed with female F_1 C57/B6 GFP mice to obtain GFP nude mice. When female F_2 immunocompetent GFP mice were crossed with male GFP nude mice, or when F_2 GFP nude male mice were back-crossed with female F_1 immunocompetent GFP mice, ~50% of their offspring were GFP nude mice. GFP nude mice can be consistently produced by the methods described above (9).

Footpad injection model. Dual-color cancer cells were washed thrice with serum-free cold medium. GFP nude mice were injected with 1×10^6 cells in a total volume of 20 μL serum-free medium into the right hind footpad. Cells were injected within 30 min of harvest (7).

Laser scanning microscope. The Olympus IV100 microscope is a scanning laser microscope. A 488-nm argon laser was used. The novel stick objectives (as small as 1.3 mm) were designed specifically for this laser scanning microscope. The very narrow objectives deliver very high resolution images (21). A PC computer running FluoView software (Olympus Corp.) was used to control the microscope. All images were recorded and stored as proprietary multilayer 16-bit Tagged Image File Format files (21).

All animal studies were conducted in accordance with the principles and procedures outlined in the *NIH Guide for the Care and Use of Animals* under assurance A3873-1. Animals were kept in a barrier facility under HEPA filtration. Mice were fed an autoclaved laboratory rodent diet (Tecklad LM-485, Western Research Products).

Results and Discussion

Noninvasive color-coded imaging of tumors at the subcellular level in the live unperturbed mouse. Tumors that developed from dual-color cancer cells in the footpad of GFP nude mice are visualized at the cellular and subcellular level in their microenvironment in Fig. 1. The cancer cells are the MMT (Fig. 1*A*) and LLC (Fig. 1*B*). The cancer cells are double-labeled expressing GFP in the nucleus and RFP in the cytoplasm. The nuclei of the cancer cells appear yellow because they are surrounded by RFP cytoplasm. The green cells are the host cells because they express GFP only. Although both tumor

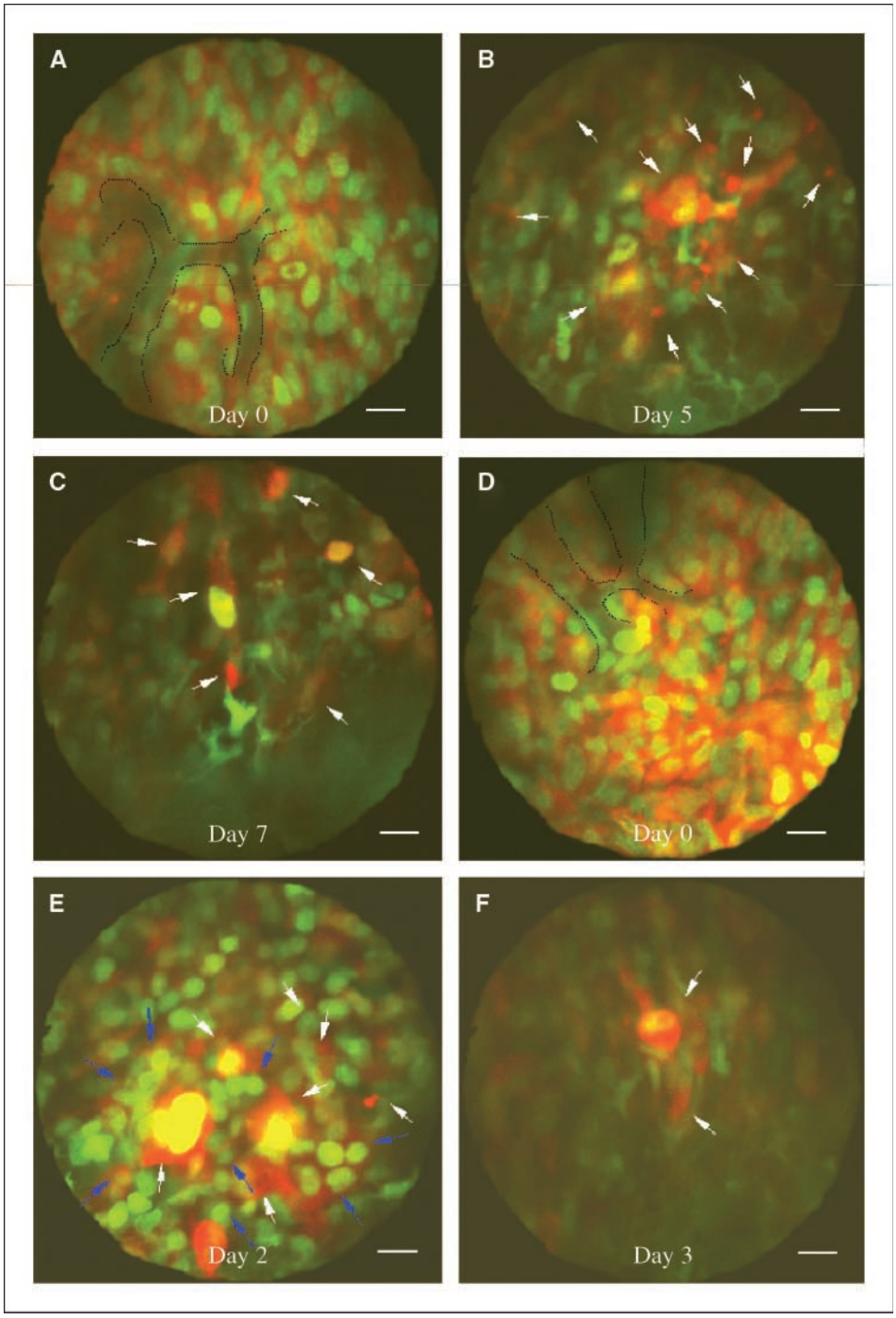

Figure 3. Whole-body, noninvasive, subcellular imaging of drug response of dual-color Lewis lung carcinoma cells and GFP stromal cells in the live GFP nude mouse. *A* to *C*, dual-color Lewis lung carcinoma cells responding to taxol. *A*, whole-body image of untreated dual-color Lewis lung carcinoma cells in the footpad of a live GFP mouse. Note the numerous highly heterogenic dual-color Lewis lung carcinoma cells interdispersed among the GFP host stromal cells. Tumor blood vessels also can be seen (*dashed black lines*). *B,* drug-induced cell death can be seen in a live GFP nude mouse day 5 after treatment with taxol (5 mg/kg). The tumor cells frequently fragmented with separation of nucleus and cytoplasm (*arrows*). *C,* the number of cancer cells was dramatically reduced by day 7 after treatment with taxol (*arrows*). *D* to *F*, dual-color Lewis lung carcinoma cells responding to cisplatin. *D,* whole-body image of untreated dual-color Lewis lung carcinoma cells in the footpad of a live GFP mouse. *E,* whole-body image of *in vivo* drug response of dual-color Lewis lung carcinoma day 2 after i.v. injection of 10 mg/kg cisplatin. Many Lewis lung carcinoma cells lost their original shape. The nuclei were condensed and the cells were dying (*white arrows*). These dying tumor cells were surrounded by lymphatic-like host cells (*blue arrows*). *F,* the number of cancer cells was dramatically reduced by day 3 after treatment with cisplatin. Only a few dying cancer cells and cell fragments can be visualized (*arrows*). *Bar,* 20 μm.

types contain numerous green stromal cells, the MMT tumor seems more enriched in stromal cells. In both tumors, cancer cells are interdispersed between the stromal cells. The stromal cells form a very significant portion of the tumor. The stromal cells seem more heterogeneous in the Lewis lung tumor. Dividing cancer cells can be visualized by their two juxtaposed nuclei. Blood vessels are prominently seen in the MMT tumor. They appear dark due to absorption of light by hemoglobin in the red cells that do not express GFP. These are the first images of tumors in the unperturbed live animal at subcellular resolution.

Noninvasive color-coded scanning imaging of unperturbed tumors in the live animal. Figure 1*C* and *D* shows the LLC-GFP-RFP tumor being scanned from the outer surface to the inner. The outer surface is mostly GFP host cells. Numerous host GFP dendritic as well as other cell types can be seen at the surface. Other stromal cells seem prominent as scans are made at 10-μm intervals. At 80-μm depth, cancer cells become more predominant. Mitotic cancer cells can be discerned by juxtaposed nuclei. Stromal cells are observed in close proximity to cancer cells throughout the tumor.

Noninvasive color-coded imaging of the effects of chemotherapy in real time on cancer and stromal cells. In the

Table 1. Efficacy of doxorubicin on cancer cells in a tumor determined by color-coded whole-body imaging

Condition	Total area of cancer cells (pixels) per field	Cancer cells/tumor (pixels) per field	Total cancer cell number per field
Before chemotherapy	54,223	54,223/194,697 (28%)	50
After chemotherapy	22,194	22,194/194,697 (11%)	28

NOTE: GFP transgenic mice were implanted with MMT cells expressing GFP in the nucleus and RFP in the cytoplasm. Mice were treated with doxorubicin and whole body imaged as described in Materials and Methods. Quantitative data were derived from Fig. 2*A* and *B*.

MMT tumor model, the cancer cells are sensitive to doxorubicin (10 mg/kg, i.v.). The cancer cells lose their spindle shape, and the nuclei tend to contract soon after treatment (Fig. 2*A* and *B*). Tumor blood vessels could be visualized in the MMT tumor in the live mouse (Fig. 2*C*). Twelve hours after treatment with doxorubicin, the cytoplasm seemed to fragment away from the tumor cells, and the number of tumor cells was significantly reduced. The GFP host stromal cells become highly elongated in some cases (Fig. 2*D*). The data in Fig. 2*A* and *B* are quantitated in Table 1. In the Lewis lung tumor, cancer cells are sensitive to taxol (5 mg/kg, i.v.) and cisplatin (10 mg/kg, i.v.). Color-coded interacting cancer and stromal cells and tumor blood vessels were imaged before chemotherapy (Fig. 3*A* and *D*). On day 5 after treatment with taxol, the cytoplasm seemed to fragment from the cancer cells (Fig. 3*B*), and the number of cancer cells was significantly reduced by day 7 after treatment (Fig. 3*C*). In the case of cisplatin, the nuclei of the cancer cells condensed. The shape of the cancer cells changed by day 2 after treatment, and they become surrounded by lymphatic-like GFP host stromal cells (Fig. 3*E*). On day 3 after treatment, the number of cancer cells was dramatically reduced (Fig. 3*F*). The three-color imaging model described here allows for the first time the ability to noninvasively observe drug response at the subcellular level in tumors in the living animal.

Noninvasive color-coded imaging of tumor blood flow before and after chemotherapy. Before treatment, numerous GFP-expressing host cells can be seen in the tumor blood flow. After treatment, the number of GFP-expressing host cells in the blood flow was greatly reduced, and RFP cytoplasmic fragments were observed, which were stripped from the cancer cells due to chemotherapy. See Supplementary Material for movies for whole-body imaging of tumor blood flow before and after chemotherapy.

The results described here are a significant improvement from the inserted-window models of Jain et al. (22) or of the skin flap models we have previously developed to image tumors (8, 23). A striking observation is the interdispersal of cancer cells among the host stromal cells in the tumor microenvironment. Such observations were made possible by using the Olympus IV100 Intravital Laser Scanning Microscope, a ubiquitously-expressing GFP mouse as a host, and cancer cells expressing RFP in the cytoplasm and GFP in the nucleus that appears yellow due to the surrounding RFP cytoplasm. We also showed the usefulness of this model to noninvasively image chemotherapy of tumors in real time at the subcellular level, which distinguishes efficacy on cancer and stromal cells. Tumor blood flow was readily imaged, and striking changes were observed after chemotherapy. The ultra-narrow objectives of this scanning imager enable the very high resolution whole-body images obtained in the present study.

The new technology described in this report enables clear color-coded distinction of cancer and stromal cells without perturbing the tumor or the animal. Future experiments will develop techniques to differentially label cancer and stromal cells in cancer patients' surgical specimens in order to transplant and image cancer cell/stromal cell interactions in patient tumors as we did for the tumor cell lines in the present study. The patient specimens will give further opportunity to screen for new drugs that specifically target stromal cells that play a critical role in tumor behavior, in particular, malignancy.

The results described here are also an improvement on the study previously done with the IV100 where the "stick" objective was inserted into the animal (21). Although this was a useful application of this instrument, the present report shows that the IV100 can be used for whole-body, completely noninvasive color-coded imaging at the subcellular level with very high resolution.

The Supplementary Movies strikingly show the power of this technology to noninvasively image color-coded cancer and stroma cells in real time in the unperturbed tumor, including tumor blood flow. This capability depends on having a model expressing multiple-colored fluorescent proteins. This new technology opens many new possibilities for studying cancer cell/stromal cell interactions in the microenvironment noninvasively at the cellular level and as a new approach for *in vivo* cell biology and drug discovery.

Acknowledgments

Received 12/13/2006; revised 2/14/2007; accepted 3/16/2007.

Grant support: National Cancer Institute grants CA103563 and CA099258 (AntiCancer).

The costs of publication of this article were defrayed in part by the payment of page charges. This article must therefore be hereby marked *advertisement* in accordance with 18 U.S.C. Section 1734 solely to indicate this fact.

References

1. Hoffman RM. The multiple uses of fluorescent proteins to visualize cancer *in vivo*. Nat Rev Cancer 2005;5:796–806.
2. Hoffman RM, Yang M. Subcellular imaging in the live mouse. Nature Protocols 2006;1:775–82.
3. Hoffman RM, Yang M. Color-coded fluorescence imaging of tumor-host interactions. Nature Protocols 2006;1:928–35.
4. Hoffman RM, Yang M. Whole-body imaging with fluorescent proteins. Nature Protocols 2006;1:1429–38.
5. Chishima T, Miyagi Y, Wang X, et al. Cancer invasion and micrometastasis visualized in live tissue by green fluorescent protein expression. Cancer Res 1997;57:2042–7.
6. Yang M, Baranov E, Jiang P, et al. Whole-body optical imaging of green fluorescent protein-expressing tumors and metastases. Proc Natl Acad Sci U S A 2000;97:1206–11.
7. Yamamoto N, Jiang P, Yang M, et al. Cellular dynamics visualized in live cells *in vitro* and *in vivo* by differential

dual-color nuclear-cytoplasmic fluorescent-protein expression. Cancer Res 2004;64:4251–6.
8. Yang M, Li L, Jiang P, et al. Dual-color fluorescence imaging distinguishes tumor cells from induced host angiogenic vessels and stromal cells. Proc Natl Acad Sci U S A 2003;100:14259–62.
9. Yang M, Reynoso J, Jiang P, et al. Transgenic nude mouse with ubiquitous green fluorescent protein expression as a host for human tumors. Cancer Res 2004;64:8651–6.
10. Yang M, Baranov E, Wang J-W, et al. Direct external imaging of nascent cancer, tumor progression, angiogenesis, and metastasis on internal organs in the fluorescent orthotopic model. Proc Natl Acad Sci U S A 2002;99:3824–9.
11. Katz MH, Bouvet M, Takimoto S, et al. Selective antimetastatic activity of cytosine analog CS-682 in a red fluorescent protein orthotopic model of pancreatic cancer. Cancer Res 2003;63:5521–5.
12. Katz MH, Bouvet M, Takimoto S, et al. Survival efficacy of adjuvant cytosine-analogue CS-682 in a fluorescent orthotopic model of human pancreatic cancer. Cancer Res 2004;64:1828–33.
13. Verkhusha V, Lukyanov KA. The molecular properties and applications of Anthozoa fluorescent proteins and chromoproteins. Nat Biotechnol 2004;22:289–96.
14. Zimmer M. Green fluorescent protein (GFP): applications, structure and related photophysical behavior. Chem Rev 2002;102:759–81.
15. Folkman J. Angiogenesis and apoptosis. Semin Cancer Biol 2003;13:159–67.
16. Paget S. The distribution of secondary growths in cancer of the breast. Lancet 1889;133:571–3.
17. Orimo A, Gupta PB, Sgroi DC, et al. Stromal fibroblasts present in invasive human breast carcinomas promote tumor growth and angiogenesis through elevated SDF-1/CXCL12 secretion. Cell 2005;121:335–48.
18. Ferrara N, Kerbel RS. Angiogenesis as a therapeutic target. Nature 2005;438:967–74.
19. Kerbel RS. A cancer therapy resistant to resistance. Nature 1997;390:335–6.
20. Chen HX, Mooney M, Boron M, et al. Phase II multicenter trial of bevacizumab plus fluorouracil and leucovorin in patients with advanced refractory colorectal cancer: an NCI Treatment Referral Center Trial TRC-0301. J Clin Oncol 2006;24:3354–60.
21. Alencar H, Mahmood U, Kawano Y, Hirata T, Weissleder R. Novel multiwavelength microscopic scanner for mouse imaging. Neoplasia 2005;7:977–83.
22. Jain RK, Munn LL, Fukumura D. Dissecting tumour pathophysiology using intravital microscopy. Nat Rev Cancer 2002;2:266–76.
23. Yamauchi K, Yang M, Jiang P, et al. Development of real-time subcellular dynamic multicolor imaging of cancer cell trafficking in live mice with a variable-magnification whole-mouse imaging system. Cancer Res 2006;66:4208–14.